

Laser Desorption and Imaging of Proteins from Ice via UV Femtosecond Laser Pulses

Jamal I. Berry,[†] Shixin Sun,[†] Yusheng Dou,[‡] Andreas Wucher,[§] and Nicholas Winograd^{*,†}

Department of Chemistry and Materials Research Institute, Pennsylvania State University, University Park, Pennsylvania 16801, Department of Physics, Texas A&M University, College Station, Texas 77843, and Institute of Experimental Physics, Duisburg-Essen University, 45117 Essen, Germany

We have employed 200-fs, 400-nm laser pulses to desorb intact protein molecular ions directly from a frozen aqueous matrix. The resulting spectra obtained using a variety of proteins varying in molecular weight from 1060 (bradykinin) to 5778 Da (insulin) are compatible with those obtained with traditional matrix-assisted laser desorption/ionization experiments. High-quality spectra could be generated using a fluence of 4.0–9.0 J/cm² to desorb proteins from an aqueous solution frozen onto metal substrates with a sensitivity in the femtomole range. Although the mechanism behind this effect is still not clear, we speculate that it involves explosive boiling of the ice layer due to rapid heating of the substrate. Imaging experiments conducted on the ice layer suggest that the yield of protein is approximately independent of the film thickness and is very reproducible from shot to shot. The results are particularly significant since they open the possibility of examining a range of biomaterials directly from the in vivo aqueous environment.

Matrix-assisted laser desorption/ionization (MALDI) is a widely used tool for mass spectrometric analysis of polymers and biomolecules.¹ The key to this technology is to find appropriate organic crystalline matrixes that absorb the incident laser energy allowing the analyte to be ejected into vacuum intact as a molecular ion. These matrixes have proven to be quite efficient in the process of desorption/ionization, allowing spectra of proteins, enzymes, DNA, RNA, and oligonucleotides of hundreds of kilodaltons to be obtained routinely with good sensitivity for a variety of applications.

A frozen aqueous solution would be an attractive matrix for MALDI-type experiments since water is a natural component of most biomaterials. Sample manipulation would be reduced, and biomolecules could be detected in their native environment (i.e., tissues and cells). When considering protein dynamics and structure, the water environment provides improvement since stable interactions may change dramatically upon cocrystallization within an acidic matrix.² Altering the native conformation of

proteins, enzymes, and DNA through denaturation would be significantly reduced upon sample freezing.³ Moreover, it is possible that effects associated with fragmentation and metastable decay could be reduced by yielding ions that have less internal energy. Finally, dissolution of the analyte molecule in water allows increased sample homogeneity, producing uniform targets with potentially higher shot-to-shot reproducibility.

Our approach to using ice as a matrix was first proposed by Nelson and co-workers, who employed nanosecond visible laser pulses for the direct assay of biomolecules from pure frozen aqueous solutions.^{4–6} While DNA molecules up to ~410 kDa were shown to desorb intact as verified by collector experiments,⁴ spectra of a lysozyme dimer at ~29 kDa and single-stranded DNA molecules up to ~18 kDa were obtained from thin frozen ice films on a corroded copper substrate.⁵ Tuning of the laser to excite sodium atoms through the D-line resonance at 598 nm was shown to enhance ionization efficiency, presumably through Na⁺ adduct formation with biomolecules in the ablated plume.⁶ Although the results are intriguing, they were not sufficiently reproducible to allow for routine studies. Subsequent approaches employing nanosecond IR lasers for assay with ice as a matrix were found to be feasible for assay of biomolecules up to 30 kDa by coupling directly into the 3- μ m O–H stretching mode of water.⁷ Although this method yields high-quality mass spectra, there are still sensitivity issues due to the large sampling depths required. Recently, IR spectra of angiotensin II (1046 Da) from an ice matrix were obtained by accessing the O–H bending mode of water and the vibrational mode of ice near 6 μ m with a picosecond free electron laser.⁸

Here we show that UV femtosecond laser pulses can be used to obtain mass spectra of proteins and potentially other biomolecules from an aqueous thin film frozen onto metal substrates

* Corresponding author. Tel: (814) 863-0001. Fax: (814) 863-0618. E-mail: nxw@psu.edu.

[†] Pennsylvania State University.

[‡] Texas A&M University.

[§] Institute of Experimental Physics.

(1) Hillenkamp, F.; Karas, M.; Beavis, R. C.; Chait, B. T. *Anal. Chem.* **1991**, *63*, 1193A–1202A.

(2) Fenn, J. B.; Mann, M.; Meng, C. K.; Wong, S. F.; Whitehouse, C. M. *Science* **1989**, *246*, 64–71.

(3) Fahy, G. M.; Lilley, T. H.; Linsdell, H.; Douglass, M. S.; Meryman, H. T. *Cryobiology* **1990**, *27*, 247–268.

(4) Nelson, R. W.; Rainbow, M. J.; Lohr, D. E.; Williams, P. *Science* **1989**, *246*, 1585–1587.

(5) Williams, P.; Chou, C. W.; Schieltz, D. M. In *Automation Technologies for Genome Characterization*; Beugelsdijk, T. J., Ed.; Wiley: New York, 1997; pp 227–254.

(6) Williams, P. *Int. J. Mass. Spectrom.* **1994**, *131*, 73–96.

(7) Berkenkamp, S.; Karas, M.; Hillenkamp, F. *P. Natl. Acad. Sci., U.S.A.* **1996**, *93*, 7003–7007.

(8) Baltz-Knorr, M. L.; Shriver, K. E.; Haglund, R. F., Jr. *Appl. Surf. Sci.* **2002**, *11*, 197–201.

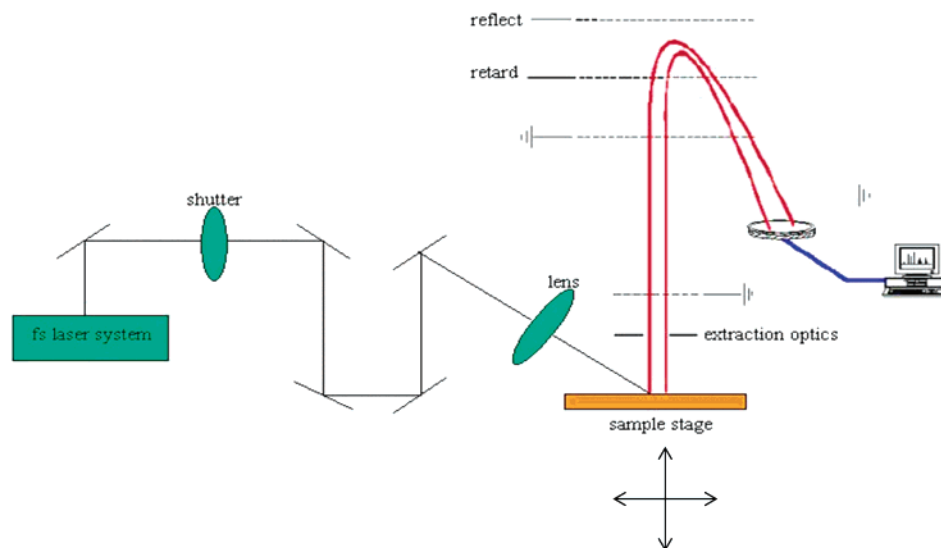


Figure 1. Schematic overview of the BIOTOF mass spectrometer modified for laser desorption experiments.

routinely and reproducibly. The idea behind this experiment is based on computer simulations^{13–15} of rapid heating of a substrate in contact with an overlayer of an enkephalin molecule embedded in an ice film. For fast heating rates, the simulations show that explosive boiling occurs in the water near the absorbing substrate followed by large clusters of water being ejected from the ice film entraining the enkephalin molecule.

EXPERIMENTAL SECTION

The Ti:sapphire femtosecond laser system (Clark-MXR, Inc.) employed in these experiments has been described previously.⁹ Briefly, the output of a self-mode locked Ti:sapphire oscillator pumped by an Ar⁺ laser (Spectra Physics) is used to seed a Ti:sapphire regenerative amplifier using chirped pulse techniques. The final output of the system produces a train of 800-nm pulses up to 1-kHz repetition rate at pulse widths of 100 fs, with 3.5 mJ/pulse. The 800-nm output is sent directly into a harmonic generator to produce 400-nm pulses with pulse energy of 0.5 mJ/pulse. The pulse width of 200 fs is determined by cross-correlation techniques. A CaF₂ lens (25-cm focal length) mounted outside the time-of-flight (TOF) mass spectrometer previously described elsewhere¹⁰ is used to focus at the sample in the analysis chamber as shown in Figure 1. The laser spot size is $\sim 50 \mu\text{m}$ in diameter as determined by direct optical measurement and by the lateral resolution observed in imaging experiments. By changing the laser pulse energy and focal length, the laser power density can

be varied over a wide range. Laser exposure to the sample surface is regulated by a high-speed shutter from Uniblitz and is interfaced for computer control during experiments.

For laser imaging experiments, stepper motors (Superior Electric) are coupled to the sample stage via micrometers with digital readout (Mitutoyo) and interfaced for computer control. An image is generated by acquiring the mass spectrum at particular coordinates on the sample (pixel) and then moving the stage via stepper motors to a sequential location to eventually map the desired field of view. Pixels are spaced by $16 \mu\text{m}$ and are interrogated by one laser shot focused to a spot of $\sim 50 \mu\text{m}$ in diameter. The field of view (i.e., effective area rastered) may be changed by adjusting the number of steps (or increments of the stepper) between pixels. Images of the same field of view can be generated with different pixel resolution by adjusting the number of stepper motor steps per pixel and the number of pixels. Spatial resolution of the image is typically limited by the laser spot size in these experiments as the stepper motors are $1.6 \mu\text{m}/\text{step}$. The laser repetition rate is chosen to be compatible with the speed of the steppers and is 80 Hz for all of the experiments reported here.

Ions desorbed are time-delayed, pulse-extracted, and accelerated into a reflecting TOF mass analyzer and are detected via a microchannel plate detector as illustrated in Figure 1.¹⁰ Time-delayed pulsed extraction is employed for higher mass resolution and detection of higher mass proteins in instances where the extraction voltage at the stage is not biased. The voltage applied to the stage or acceleration potential is 2500 eV for positive ions. Ions were detected after postacceleration to 23 keV (Kore Technologies). A digital-to-analog converter (Signatec) PDA 500 is used with 2-ns resolution to measure the signal from the detector.

Proteins are obtained from Sigma/Aldrich and used without further purification. Femtomole sensitivity is easily obtained from the frozen aqueous solutions via laser desorption/ionization (LDI). Samples were prepared by dissolving 1 mg ($\sim 1 \mu\text{mol}$) of protein in 1 mL of a 50:50 acetonitrile/water solution acidified with 0.1% trifluoroacetic acid (TFA). Sample solutions are mixed with 1/3 volume ethanol to prepare thin aqueous films on the substrate

- (9) Willey, K. F.; Vorsa, V.; Braun, R. M.; Winograd, N. *Rapid Commun. Mass Spectrom.* **1998**, *12*, 1253–1260.
- (10) Braun, R. M.; Blenkinsopp, P.; Mullock, S. J.; Corlett, C.; Willey, K. F.; Vickerman, J. C.; Winograd, N. *Rapid Commun. Mass Spectrom.* **1998**, *12*, 1246–1252.
- (11) Juhasz, P.; Costello, C. E.; Biemann, K. *J. Am. Soc. Mass Spectrom.* **1993**, *4*, 399–409.
- (12) Westmacott, G.; Ens, W.; Hillenkamp, F.; Dreisewerd, K.; Schurenberg, M. *Int. J. Mass Spectrom.* **2002**, *221*, 67–81.
- (13) Dou, Y.; Zhigilei, L. V.; Postawa, Z.; Winograd, N.; Garrison, B. J. *Nucl. Instrum. Methods Phys. B* **2001**, *180*, 105–111.
- (14) Dou, Y.; Zhigilei, L. V.; Winograd, N.; Garrison, B. J. *J. Phys. Chem. A* **2001**, *105*, 2748–2755.
- (15) Dou, Y.; Winograd, N.; Garrison, B. J.; Zhigilei, L. V. *J. Phys. Chem. B* **2003**, *107*, 2362–2365.

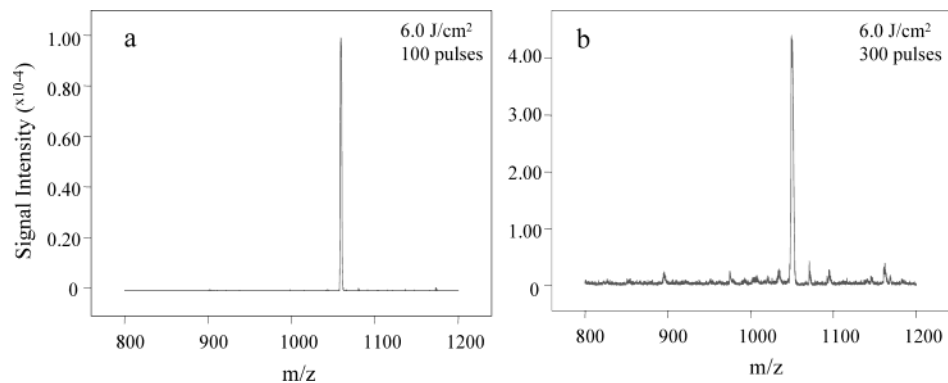


Figure 2. Laser desorption spectra of 1 mg/mL bradykinin (1060 Da) in H₂O/acetonitrile and 0.1%TFA frozen on Au at (a) 100 and (b) 300 pulses (6.0 J/cm²).

held to the sample block via gold fingers. The samples are quickly frozen by suspending the block containing the mounted sample substrate in liquid nitrogen. After freezing, the samples are immediately transferred to the fast entry port and evacuated for ~30 s with a sorption pump before being introduced into the preparation chamber. The sample block (i.e., copper stub) is then transferred into the sample analysis chamber when a pressure of $\sim 5.0 \times 10^{-8}$ Torr is achieved and held in place by a cold stage cooled by liquid nitrogen to 100 K as previously described.¹⁰

Silicon wafers are obtained from Silicon Quest International (Santa Clara, Ca). Gold substrates are prepared by vapor deposition of 2000 Å of 99.99% pure gold wire obtained from Refining Systems Inc. (Las Vegas, NV) on Si wafers coated with 100 Å of Cr. Silver and indium foil substrates are obtained from Sigma. Copper spectra are recorded directly from frozen ice samples on the Cu stub (block) used for sample analysis. All substrates are cleaned with hexane followed by rinsing in ethanol and dried under a stream of nitrogen. Before rinsing with solvent, the Cu stub is cleaned thoroughly with Scotchbrite to remove oxidation.

For our first attempts to create samples, protein was dissolved in a 50:50 mixture of an acetonitrile/H₂O solution. The solution was deposited on the Au substrates and fast frozen by dipping in liquid nitrogen. This method of preparation yields relatively "thick" samples due mainly to the surface tension of water, which prevents wetting of the substrate. This procedure does not yield meaningful protein mass spectra. Reproducible results are achieved, however, by utilizing an equal mixture of acetonitrile, H₂O, and ethanol. The addition of ethanol decreases the surface tension of the aqueous solution, allowing the creation of a much thinner ice film after freezing. Optimization of conditions produces frozen samples that are visually thin, allowing the incident laser energy to be absorbed more efficiently by the sample substrate.

RESULTS AND DISCUSSION

To generate spectra, frozen samples were irradiated with the laser while rapidly moving (scanning) the sample stage in the analyzed area. In this manner, spectra were routinely obtained from the sample edge (i.e., the thinnest portion) working toward the center of the frozen drop. The mass spectra of bradykinin from frozen aqueous solution on a gold substrate are shown in Figure 2. Spectra of very good quality were obtained as shown in Figure 2a. The presence of adduct formation with ions such as Na or K typically encountered with traditional matrixes is

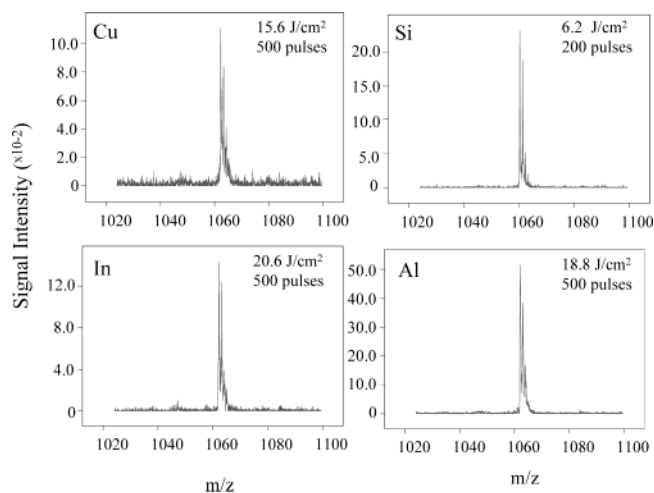


Figure 3. Laser desorption spectra of bradykinin on (a) Cu (15.6 J/cm², 500 pulses), (b) Si (6.2 J/cm², 200 pulses), (c) In foil (20.6 J/cm², 500 pulses), and (d) Al (18.8 J/cm², 500 pulses) substrates.

significantly reduced.¹¹ Only when the sample is irradiated for longer times are the presence of adducts observed to form as illustrated in Figure 2b.

Since the laser energy at 400 nm is not absorbed by the frozen overlayer, but primarily by the substrate as previously noted, spectra on a variety of different substrates were recorded to determine the efficacy of this technique. As shown in Figure 3, spectra of bradykinin are routinely obtainable from frozen samples on substrates of Si, Cu, In, and Al. These spectra are particularly fascinating in that they illustrate the potential and open the possibility of obtaining protein signals from frozen overlayers on any number of metal and other substrates.

It is essential to determine the laser fluence that yields the highest quality mass spectra. The spectrum of a thin film of melittin in aqueous solution and frozen on Au substrate is shown in Figure 4a. The presence of M²⁺ can be seen in the spectrum as typically observed in MALDI when UV-absorbing matrixes are used.¹¹ Moreover, no Na⁺ or K⁺ adduct ions are detected even though the sample has not been pretreated by traditional desalting protocols. A spectrum recorded at twice the fluence used in Figure 4a is shown in Figure 4b for comparison. The presence of Au clusters up to 7000 Da is indicative of the relatively thin nature of the ice film. The presence of Au clusters is not observed in Figure 4a. The spectrum of insulin shown in Figure 4c is recorded at

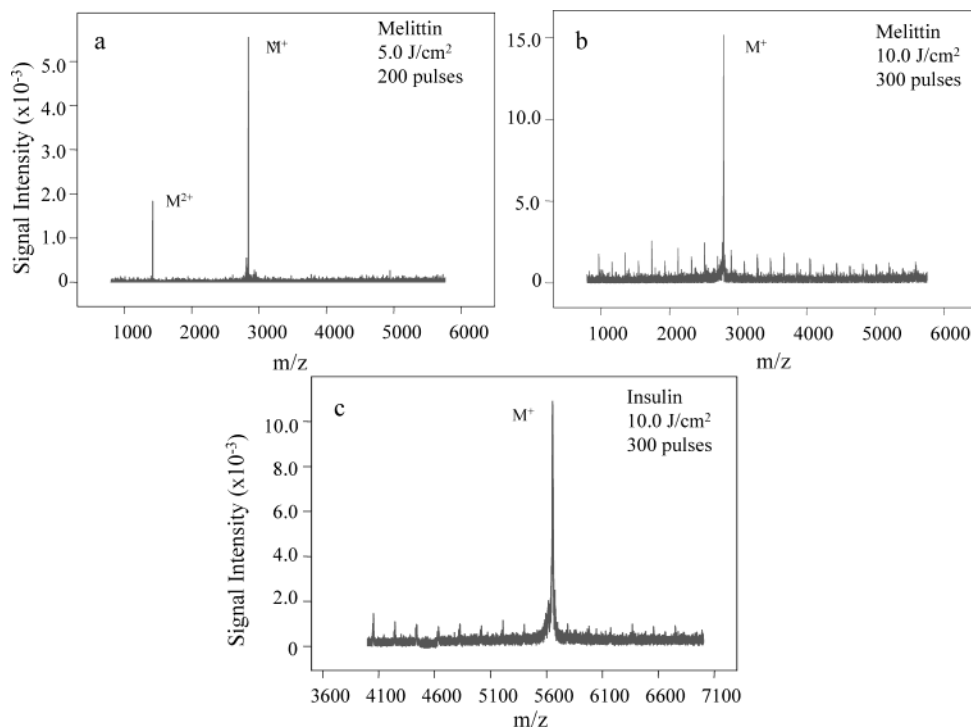


Figure 4. Laser desorption spectrum of melittin (2817 Da) from bee venom on Au at (a) 200 pulses, 5 J/pulse, and (b) 300 pulses, 10 J/pulse. (c) Spectrum of insulin from porcine pancreas (300 pulses, 10 J/pulse, 5778 Da). The presence of Au clusters can be seen throughout the spectra in (a) and (c).

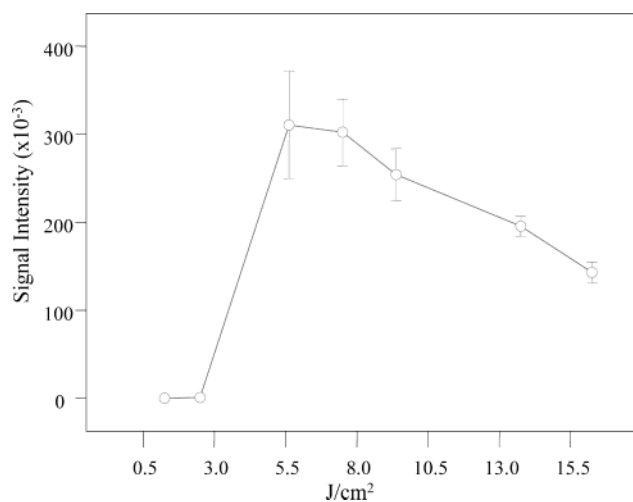


Figure 5. Bradykinin signal intensity vs laser fluence at 400 nm from ice overlayer on Au substrate. Data points were recorded with 15 laser shots. Laser spot size is 50 μm .

the same fluence as that shown in Figure 4b and similarly reveals the presence of high molecular weight Au clusters. The slightly higher fluence (10 J/cm²) is significant enough to cause evaporation of the Au overlayer on the substrate upon irradiation as can be seen visually and verified spectrally, penetrating into the Cr/Si sublayer.

The effect of laser fluence on the bradykinin signal intensity from ice on a Au substrate is depicted in Figure 5. At low fluence, very little bradykinin signal is observed, until a threshold of ~ 2.0 J/cm² is reached. Signal intensity then significantly jumps to maximum at ~ 5.5 J/cm², and then steadily decreases with increasing fluence. This fluence dependence is qualitatively similar to that reported in MALDI experiments.¹² At a moderately high

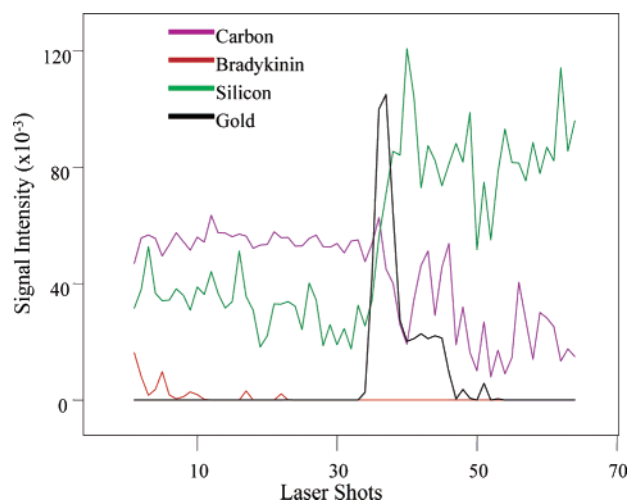


Figure 6. Signal intensity vs laser shot for bradykinin, gold, carbon, and silicon. Spectra were recorded at a fluence of 4.0 J/cm².

fluence (~ 9.0 J/cm²), the presence of Au clusters is observed as shown previously in Figure 4b and c.

To determine the effects of multiple laser pulses on the bradykinin signal intensity, spectra from the same irradiation area were obtained at an optimum fluence of 5.0 J/cm². As depicted in Figure 6, the signal from bradykinin is obtained during the first 22 laser shots with a maximum intensity found during the first pulse. Relatively high signal intensity is also observed for carbon at m/z 12, which maintains a relatively constant signal for the first 30 shots. The presence of this carbon signal is coincident with the signal associated with the bradykinin overlayer. When this carbon signal intensity decreases, the gold intensity reaches a maximum value. This observation suggests that the protein overlayer is removed, exposing the gold overlayer on the

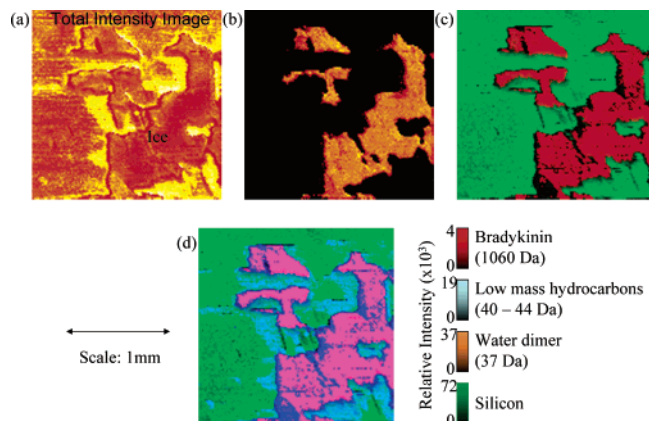


Figure 7. Laser desorption image of bradykinin in ice. Field of view is 2 mm (128×128 pixels) for all images. Intensity scales for each species are indicated by the accompanying color bars. (a) Total intensity image of sample area analyzed for bradykinin. (b) $(\text{H}_2\text{O})_2\text{H}^+$ ($m/z = 37$) image. (c) Image of bradykinin signal intensity depicted in red and Si substrate intensity as green. (d) Image of Si substrate in green, bradykinin in red, and low-mass hydrocarbon signal intensity from m/z 40 to 44 shown as blue. The original film exhibited uniform distribution of bradykinin. This image exhibits regions of high and low concentrations of bradykinin since portions of the film have been removed by prior laser ablation experiments.

substrate. Upon the abrupt depletion of gold, the silicon signal intensity then plateaus to its maximum value for the remaining duration of laser exposure. For this configuration, a single laser shot does not remove the entire ice overlayer, leaving a residual ice film available for interrogation by subsequent laser pulses.

We find that solvation is important for the detection of analyte molecules. Experiments with dried protein films on Au substrates at 100 K yield no measurable protein signal. A decrease in the survival of the protein is expected in this environment given the close proximity to the interface and the extremely high temperatures reached upon substrate heating. Since the analyte is in direct contact with the interface, the temperature brought about upon substrate heating may decrease analyte survival. The presence of Au clusters is similarly not observed in experiments in which the analyte solution is prepared as a dried film.

To ascertain the lateral distribution of analyte signal, LDI-MS images of the samples were obtained. The total intensity ion image is shown in Figure 7a. Islands of frozen aqueous sample can be seen on the target area. To depict water, the dimer at m/z 37 is mapped in the image as shown in Figure 7b. The presence of the $(\text{H}_2\text{O})_2\text{H}^+$ signal intensity is brightest in the area of the frozen sample (yellow regions). The bradykinin signal intensity is shown in Figure 7c and is represented by the color red with silicon ions shown as green. As can be seen in the image, the analyte signal is localized to regions of the sample where $(\text{H}_2\text{O})_2\text{H}^+$ or ice is present.

The lateral distribution of low-mass fragment ions is illustrated in Figure 7d. The bradykinin signal intensity (red) is mapped with low-mass hydrocarbons in the region m/z 40–44. The presence of low-mass hydrocarbons in regions of ice where the bradykinin signal is present causes the image to be purple. Areas along the edge of the frozen sample exhibit no protein signal and correspond to regions in which the low-mass hydrocarbon signal is highest in intensity. Blue areas in which the low-mass hydrocarbons extend from the frozen sample are also observed. Their origin is

currently unknown. These images suggest that the sample protocol used here may find important bioanalytical applications, since target molecules may be localized directly from a frozen hydrated biological environment without having to dope the sample with a MALDI-style matrix. Moreover, the lateral resolution of these images is $\sim 20 \mu\text{m}$, a value somewhat smaller than the laser probe size of $\sim 50 \mu\text{m}$. Hence, it may well be feasible with sharper optical focus to achieve lateral resolution of $1 \mu\text{m}$.

It is premature to present a full picture of the mechanism of this unique set of observations. There are several features of the experimental configuration, however, which suggest that specific physical phenomena are playing a role in allowing desorption of intact protein molecules. The most interesting feature of the experiment is, of course, the fact that the laser energy is absorbed primarily by the metal substrate and not by the ice–protein overlayer. This situation is in sharp contrast to MALDI where the UV-absorbing organic crystal host acts as the energy absorber.

Laser ablation of ice films on metal substrates using ultrashort laser pulses has recently been modeled using molecular dynamics (MD) computer simulations.^{13,14} Huge water clusters are shown to be ejected from metal surfaces when Au is heated on the picosecond time scale, whereas smaller water clusters are observed in the nanosecond time regime.¹⁵ The ejection of huge water clusters is attributed to the rapid heating of the Au substrate and subsequent explosive boiling at the Au/water interface.

More recent MD simulations of substrate heating with an ice overlayer containing the small molecule enkephalin reveal that liftoff of the enkephalin molecule¹⁵ is more feasible using shorter laser pulses and more rapid heating of the substrate. Though modeled at lower energy (fluence) and longer pulse widths than those used for the experiments presented in this work, the MD simulations may provide some insight into the mechanism for desorption.

Finally, we believe that the presence of the ice layer provides an evaporative cooling bath that may stabilize the protein molecules during the desorption event. This effect is illustrated by the observation of gold clusters containing up to 45 atoms.¹⁶ These clusters are only observed when the ice layer is present. Hence, the layer must provide a favorable environment for the formation of large molecular species.

CONCLUSIONS

We have demonstrated for the first time that protein signals can be observed repeatedly and routinely from an ice matrix via UV LDI with femtosecond laser pulses. Though the complete mechanism of this unique approach is yet unclear, we hypothesize that it involves rapid heating of the sample substrate within short time scales and the explosive boiling and subsequent liftoff of huge water clusters with the embedded analyte as revealed by recent MD simulations. The presence of an ice overlayer stabilizes the ejection of intact molecular ions as assays of dried protein films in the absence of ice overlayers reveal no analyte signal. This observation suggests that an evaporative cooling of the entrained molecule may occur during desorption. These experiments have also been performed on a variety of different substrates and illustrate the potential for obtaining protein signals from frozen overlayers on other metal substrates or surfaces. Sample homo-

(16) Berry, J.; Sun, S.; Winograd, N. Manuscript in preparation.

geneity is high, allowing molecular maps that reveal a uniform distribution of protein analyte signal from the ice overlayer. The capability of laser desorption imaging of proteins from frozen aqueous overlayers allows for future exploration of molecular imaging of tissue and cells.

ACKNOWLEDGMENT

The financial support of the National Institutes of Health (NIH) and the National Science Foundation (NSF) are gratefully ac-

knowledged. The authors appreciate the comments of Barbara Garrison, Dan Jones, and Peter Williams during the preparation of this work.

Received for review April 11, 2003. Accepted July 18, 2003.

AC034375P